

Synthesis, Structure, and Physical Properties of a Novel Quaternary Niobium Telluride, $\text{Nb}_2\text{FeCu}_{0.35}\text{Te}_4$

Jing Li,* Frank McCulley, and Mark J. Dioszeghy

Department of Chemistry, Rutgers University, Camden, New Jersey 08102-1634

S. C. Chen, K. V. Ramanujachary, and M. Greenblatt*

Department of Chemistry, Rutgers University, Piscataway, New Jersey 08855-0939

Received June 16, 1993*

$\text{Nb}_2\text{FeCu}_{0.35}\text{Te}_4$, the first solid-state quaternary niobium telluride, was prepared via chemical vapor transport reactions. The structure of this compound was determined by single-crystal X-ray diffraction methods. It crystallizes in the orthorhombic system, space group $Pmnm$ (No. 59). The unit cell dimensions are $a = 12.576(1)$ Å, $b = 3.8395(6)$ Å, $c = 7.3012(9)$ Å, $Z = 2$, and $V = 352.54(8)$ Å³. Structural refinement with 433 observed reflections ($I > 3\sigma(I)$) and 40 variable parameters results in $R = 4.0\%$ and $R_w = 4.8\%$. $\text{Nb}_2\text{FeCu}_{0.35}\text{Te}_4$ represents a novel three-dimensional structure type with interesting structural features and one-dimensional extended metal–metal bonds. The structure can be described as constructed from “ $\text{Nb}_4\text{Fe}_2\text{Cu}_2\text{Te}_{11}$ ” building units. These building units stack on top of each other along the crystallographic b -axis to form a one-dimensional chain. The interchain connections are made through Cu–Te(3) bonds along the c -axis and Nb–Te(3) bonds along the a -axis resulting in a three-dimensional network with open channels running along the b -axis. The one-dimensional metal–metal bonds extend along the b -axis. A positional disorder was observed for both Nb and Fe sites, and all three metal atoms are partially occupied. $\text{Nb}_2\text{FeCu}_{0.35}\text{Te}_4$ shows degenerate semiconductor behavior with a room-temperature resistivity of $3.6(2) \times 10^{-3}$ Ω-cm and an antiferromagnetic ordering at 8 K. The temperature-dependent magnetic susceptibility follows modified (nonlinear) Curie–Weiss behavior with $\mu_{\text{eff}} = 1.26 \mu_B$.

Introduction

Solid-state materials are often prepared at intermediate or high temperatures. The high-temperature conditions are required for a significant diffusion process to occur among the solid reactants. Molten salt¹ and chemical vapor transport (CVT)² reactions are by far the two most important and commonly used methods for crystal growth under these temperatures. For example, crystals of most binary transition metal chalcogenides² and a number of ternary compounds not containing alkali and alkaline-earth metals³ were grown by the CVT technique. Recently, the molten salt (flux) technique has also been applied to the synthesis of alkali metal and/or alkaline-earth metal containing chalcogenides.^{4,5}

The continued exploration of transition metal chalcogenides has led to the discovery of many new, interesting materials. The

binary compounds have been studied most intensively, mainly due to their various unusual properties and potential technological applications.⁶ Recently, interest in the ternary systems has also grown, and this has resulted in a considerable number of papers in the literature.³ Many of these ternary compounds show unusual structural features that deserve further investigations. Although very little is known about quaternary chalcogenide compounds, exploratory investigations are being made on the sulfide and selenide families. Several quaternary chalcogenides that contain Cu and alkali metals^{5a} or Cu/Ag and alkaline-earth metals^{5b} have been prepared via the molten salt technique.

Our search for novel materials has been mainly focused on the telluride systems, for they are relatively less studied compared to the corresponding sulfides. Many telluride compounds are indeed structurally and chemically different from the sulfides.³ The compounds that particularly interest us are the metal-rich telluride families, most of which show interesting structural features, for example, unusual metal networks containing strong metal–metal bonds.^{3e–g,i–j} We have recently succeeded in crystallizing a number of ternary group-V transition metal tellurides by employing the chemical vapor transport method.^{3e–h} In this paper, we report the synthesis and structure, as well as the magnetic and electrical properties, of $\text{Nb}_2\text{FeCu}_{0.35}\text{Te}_4$, the first solid-state

* To whom correspondence should be addressed.

• Abstract published in *Advance ACS Abstracts*, April 1, 1994.

- (1) Elwell, D.; Scheel, H. J. *Crystal Growth from High-Temperature Solutions*; Academic Press: London, 1975. Mamantov, G. *Molten Salts: Characterization and Analysis*; Marcel Dekker: New York, 1969.
- (2) Schäfer, H. *Chemical transport reactions*; Academic Press: New York, 1964. Rosenberger, F. In *Preparation and Characterization of Materials*; Ronig, J. M., Rao, C. N. R., Eds.; Oxford University Press: Oxford, U.K., 1987.
- (3) See for example: (a) Liimatta, E. W.; Ibers, J. A. *J. Solid State Chem.* **1989**, *78*, 7. (b) Halet, J.-F.; Hoffmann, R.; Tremel, W.; Liimatta, E. W.; Ibers, J. A. *Chem. Mater.* **1989**, *1*, 451. (c) Mar, A.; Ibers, J. A. *J. Solid State Chem.* **1992**, *31*, 1050. (d) Li, J.; Hoffmann, R.; Badding, M. E.; DiSalvo, F. J. *Inorg. Chem.* **1990**, *29*, 3943. (e) Badding, M. E.; DiSalvo, F. J. *Inorg. Chem.* **1990**, *29*, 3953. (f) Li, J.; Badding, M. E.; DiSalvo, F. J. *Inorg. Chem.* **1992**, *31*, 1050. (g) Badding, M. E.; Li, J.; DiSalvo, F. J.; Zhou, W. *J. Solid State Chem.* **1992**, *100*, 313. (h) Li, J.; Badding, M. E.; DiSalvo, F. J. *J. Less-Common Met.* **1992**, *184*, 257. (i) Tremel, W. *Angew. Chem., Int. Ed. Engl.* **1991**, *30*, 840. (j) Tremel, W. *Angew. Chem., Int. Ed. Engl.* **1992**, *31*, 217.
- (4) Sunshine, S. A.; Kang, D.; Ibers, J. A. *J. Am. Chem. Soc.* **1987**, *109*, 6202. Sanjines, R.; Berger, H.; Levy, F. *Mater. Res. Bull.* **1988**, *23*, 549. Kang, D.; Ibers, J. A. *Inorg. Chem.* **1988**, *27*, 549. Kanatzidis, M. G.; Park, Y. *J. Am. Chem. Soc.* **1989**, *111*, 3767. Kanatzidis, M. G. *Chem. Mater.* **1990**, *2*, 99. Park, Y.; Kanatzidis, M. G. *Angew. Chem., Int. Ed. Engl.* **1990**, *29*, 914.

- (5) (a) Lu, Y.-J.; Ibers, J. A. *J. Solid State Chem.* **1991**, *94*, 381. Keane, P. M.; Lu, Y.-J.; Ibers, J. A. *Acc. Chem. Res.* **1991**, *24*, 223. Lu, Y.-J.; Ibers, J. A. *Inorg. Chem.* **1991**, *30*, 3317. Lu, Y.-J.; Ibers, J. A. *J. Solid State Chem.* **1992**, *98*, 312. (b) Wu, P.; Christuk, A.; Ibers, J. A. Presented at the 205th National Meeting of the American Chemical Society, 1993; Abstract No. 424.
- (6) See, for example: DiSalvo, F. J.; Rice, T. M. *Phys. Today* **1979**, 32. Fleming, R.; Grimes, C. C. *Phys. Rev. Lett.* **1979**, *42*, 1423. Schollhorn, R.; Schramm, W.; Fenske, D. *Angew. Chem., Int. Ed. Engl.* **1980**, *19*, 492. Thomson, R. E.; Walter, U.; Ganz, E.; Clarke, Ishihara, Y.; Nakada, I. *Solid State Commun.* **1983**, *45*, 129. Rouxel, J. R. *Brec. Ann. Rev. Mater. Sci.* **1986**, *16*, 137. Huan, G.; Greenblatt, M. *Mat. Res. Bull.* **1987**, *22*, 505; **1987**, *22*, 943. Zettl, J. A.; DiSalvo, F. J.; Rauch, P. *Phys. Rev. B* **1988**, *38*, 10734.

quaternary niobium telluride prepared via chemical vapor transport reactions.

Experimental Section

Synthesis. Single crystals of $\text{Nb}_2\text{FeCu}_{0.35}\text{Te}_4$ were grown from chemical vapor transport reactions at 870–880 °C. A 1-g mixture of Nb (99.98%, Strem Chemicals, Inc., Newburyport, MA), Fe (99.999%, AESAR/Johnson Matthey Inc., Ward Hill, MA), Cu (99.9%, Strem Chemicals, Inc., Newburyport, MA), and Te (99.999%, Aldrich Chemical Co., Milwaukee, WI) with a molar ratio of Nb:Fe:Cu:Te = 2:1:1:4 was loaded into a 6-in. long, 10-mm i.d. quartz tube. Approximately 10 mg of the transport agent, TeCl_4 , was added to the reaction tube in a drybox. The tube was then sealed under vacuum. The reaction temperature was brought up to 875 °C within 10 h, and the sample was kept at this temperature for 2 weeks under a temperature gradient of $\Delta T = 65$ °C. After slow cooling of the furnace to room temperature, long, needle-shaped crystals were observed at the cool end of the reaction vessel. These crystals have metallic luster and did not show any sign of decomposition after standing in air for a long period of time.

Single-phase polycrystalline samples of $\text{Nb}_2\text{FeCu}_{0.35}\text{Te}_4$ were prepared at 850 °C. Stoichiometric mixtures of Nb, Fe, Cu, and Te were weighed and sealed under vacuum in a 5-in. long silica tube. The tube was heated to 850 °C within 10 h and was kept at this temperature for 3 days. Black, fine powders were formed under these conditions. No apparent attack of the reaction tube was observed. The powder X-ray diffraction pattern of this sample gave an almost perfect match with the theoretical pattern calculated by LAZY⁷ using the single-crystal data.

Microprobe analysis with a Joel JXA-8600 Superprobe on a number of selected crystals indicated the presence of all four elements: Nb, Fe, Cu, and Te in the approximate atomic ratio of 2:1:0.4:4. The more accurate composition was later established by the single-crystal X-ray structural refinement.

Physical Properties Measurement. The samples used for the resistivity measurement were in the form of rectangular bars cut from sintered pellets. The resistivity was measured in a standard four-probe configuration with a closed-cycle cryostat (APD Cryogenics, Model DE 202) in the temperature range 20–300 K. Ohmic contacts to the sample were made by attaching molten indium ultrasonically. Current–voltage profiles were recorded at different temperatures to ensure the ohmic nature of the contacts during the measurement. A SQUID magnetometer (MPMS, Quantum design) was used to measure the magnetic susceptibility of the sample in the temperature range 2–380 K in an applied magnetic field of 1000 G.

Structure Determination. A crystal with approximate dimensions of $0.12 \times 0.03 \times 0.02$ mm³ was selected for single-crystal X-ray crystallographic study. The preliminary lattice parameters were determined from oscillation and Weissenberg photographs. The final unit cell parameters and the orientation matrix for data collection were measured from least-squares analysis of the setting angles of 25 carefully centered reflections in the range $13.6^\circ \leq 2\theta \leq 27.6^\circ$. The intensity measurements were collected with an Enraf-Nonius CAD4 diffractometer at room temperature. Graphite-monochromated Mo $K\alpha$ radiation was employed to collect data with $4^\circ \leq 2\theta \leq 60^\circ$. A scan mode of $\omega-2\theta$ was used. Three standard reflections measured every 2 h showed no apparent decay in intensity during the data collection. The intensity data were corrected for Lorentz–polarization effects. The linear absorption coefficient for Mo $K\alpha$ is 229.26 cm⁻¹. An empirical absorption correction was thus applied, based on azimuthal scans of three reflections with transmission factors in the range from 0.593 to 0.998. A correction for secondary extinction was also applied in the structural refinement. A total of 607 unique reflections were collected in the octant (h,k,l), of which 433 reflections with $I > 3\sigma(I)$ were considered as observed and used in the subsequent structural solution and refinement.

The space group $Pmnm$ (No. 59) (origin choice 2)⁸ was chosen on the basis of the statistical analysis of intensity distribution and the systematic absences. Prior to the structure determination, the nonstandard cell of $Pmnm$ was transformed to the standard $Pmnm$ with the following systematic absences: $hk0, h + k \neq 2n$; $h00, h \neq 2n$; $0k0, k \neq 2n$. The

Table 1. Crystallographic Data for $\text{Nb}_2\text{FeCu}_{0.35}\text{Te}_4$

empirical formula	$\text{Nb}_2\text{FeCu}_{0.35}\text{Te}_4$	<i>f</i> _w	774.30
space group	$Pmnm$ (No. 59)	<i>T</i> (°C)	20
<i>a</i> (Å)	12.576(1)	λ (Å)	0.710 69
<i>b</i> (Å)	3.8395(6)	ρ_{calcd} (g/cm ³)	7.2944
<i>c</i> (Å)	7.3012(9)	μ (cm ⁻¹)	229.26
<i>V</i> (Å ³)	352.54(8)	<i>R</i> ^a (%)	4.0
<i>Z</i>	2	<i>R</i> _w ^b (%)	4.8

$$^a R = \sum(|F_o| - |F_c|) / \sum(|F_o|). \quad ^b R_w = [\sum w(|F_o| - |F_c|)^2 / \sum w|F_o|^2]^{1/2}, \quad w = 1/(\sigma^2(F_o)).$$

structure was solved by direct methods (SHELXS-86)⁹ and refined on $|F|$ by using the full-matrix least-squares techniques in the MolEN program package.¹⁰ Because the Fe and Cu scattering factors are close to each other, as are their bond distances to Te, the criterion used to distinguish Fe from Cu was based on the intensity analysis of the difference Fourier map, which was then correlated to the relative atomic ratio of Fe/Cu estimated from the microprobe elemental analysis. With three Te, one Nb, and one Fe atoms, the structure was isotropically refined to $R = 0.176$ and $R_w = 0.243$. Because of the large isotropic thermal parameters (B_{eq}) of the Nb (2.48 Å²) and Fe (3.70 Å²) atoms, the refinement on the occupancy of these two atoms was then applied to give $R = 0.153$ and $R_w = 0.196$ with the occupation number of 0.94 at Nb and that of 0.42 at Fe. At this stage, an electron density peak of 6.6 e/Å³ with a distance of 2.3 Å to the Te(1) atom was found in the difference map. The Cu atom was then assigned to this position. The subsequent isotropic refinement resulted in $R = 0.146$ and $R_w = 0.184$ with the occupancies of 0.48, 0.50, and 0.20 for Nb, Fe, and Cu, respectively. A θ -dependent absorption correction following the DIFABS procedure¹¹ was applied to this isotropically refined structure. The maximum and minimum correction factors were 1.17 and 0.48, respectively. The structure was then anisotropically refined to $R = 0.052$ and $R_w = 0.067$. At this point, the thermal ellipsoid of the Nb atom located at the 4*f* site (0.629, 0.75, 0.422) was highly extended along the *b*-axis ($U_{11} = 0.018$, $U_{22} = 0.126$, $U_{33} = 0.006$) with an isotropic factor (B_{eq}) of 3.95 Å². Analysis of the difference Fourier map calculated without this Nb atom led to the relocation of the Nb atom to the 8*g* site (0.629, 0.678, 0.422) or its symmetry-related position (0.629, 0.822, 0.422). These two symmetry-related positions are only 0.55 Å apart from each other, suggesting a positional disorder of the Nb atoms about the 4*f* site in the [010] direction. Based on 433 observed reflections and 40 variable parameters, the structure with the new Nb position was anisotropically refined to $R = 0.040$ and $R_w = 0.048$. The secondary extinction coefficient was 1.657×10^{-7} . The final electron density difference map was flat with a maximum of 3.01 e/Å³ and a minimum of -2.34 e/Å³ close to Te(1). The final occupancies of the metal atoms are 0.478 for Nb, 0.496 for Fe, and 0.174 for Cu, resulting in a stoichiometry of $\text{Nb}_{1.91}\text{Fe}_{0.99}\text{Cu}_{0.35}\text{Te}_4$, which is then idealized as $\text{Nb}_2\text{FeCu}_{0.35}\text{Te}_4$, consistent with the microprobe analysis. However, it is possible that Cu and Fe are disordered over the two types of sites.

The intensity data were also tested with the noncentrosymmetric model, space group $Pm2_1$ (No. 31). The structural refinement based on this model did not reach a residual index below $R = 0.10$, which further confirmed the correct choice of space group $Pmnm$ (No. 59) for the title compound.

Selected X-ray crystallographic data of $\text{Nb}_2\text{FeCu}_{0.35}\text{Te}_4$ are presented in Table 1. The final positional and isotropic thermal parameters of atoms are given in Table 2. Selected bond distances are listed in Table 3.

A supercell with doubling of the *b*-axis was also observed in oscillation and Weissenberg photographs of a large single crystal ($\sim 0.9 \times 0.1 \times 0.05$ mm³) exposed to Cu $K\alpha$ radiation with a Ni filter. The photographs were taken with a Huber Weissenberg camera.

Results and Discussion

Structure. $\text{Nb}_2\text{FeCu}_{0.35}\text{Te}_4$ represents a unique and complicated three-dimensional (3D) structure. The Nb, Fe, and Cu sites are partially occupied, as shown in Table 2. If all the metal ion sites were fully occupied, the basic building unit of the structure

(7) A program used to calculate theoretical X-ray and neutron diffraction powder patterns, written by C., Yvon, W., Jeitschko, and E. Parthé. See: *J. Appl. Crystallogr.* 1977, 10, 73.

(8) Hahn, T. *International Tables for Crystallography*; D. Reidel Publishing Co.: Dordrecht, The Netherlands, 1983; Vol. A, p 282.

(9) Sheldrick, G. M. In *Crystallographic Computing 3*; Sheldrick, G. M., Kruger, C., Goddar, R., Eds.; Oxford University Press: Oxford, U.K., 1985; pp 175–189.

(10) Fair, C. K. MolEN, Enraf-Nonius, Delft Instruments X-Ray Diffraction BV, Rontgenweg 1, 2624 BD Delft, The Netherlands, 1990.

(11) Walker, N.; Stuart, D. *Acta Crystallogr.* 1983, A39, 158.

Table 2. Atomic Coordinates and B_{eq}^a Values for Nb₂FeCu_{0.35}Te₄

atom	posn	occ ^b	x	y	z	B_{eq} (Å ²)
Te(1)	2a	1.00	0.750	0.750	0.0846(2)	1.53(3)
Te(2)	2b	1.00	0.750	0.250	0.6399(2)	1.07(2)
Te(3)	4f	1.00	0.49504(8)	0.250	0.2520(2)	1.59(2)
Nb	8g	0.478(3)	0.6289(1)	0.6783(5)	0.4222(3)	1.23(4)
Cu	4f	0.174(3)	0.559(1)	0.750	0.066(2)	2.0(2)
Fe	4f	0.496(3)	0.2058(3)	0.750	0.7007(6)	1.14(7)

^b $B_{eq} = 8\pi^2/3 \sum U_{ij} a_i^* a_j^* a_i a_j$, where the temperature factors are defined as $\exp(-2\pi^2 \sum h_i h_j a_i^* a_j^* U_{ij})$. ^c Space group *Pmmn* (No. 59), origin choice 2.

Table 3. Selected Interatomic Distances (Å) for Nb₂FeCu_{0.35}Te₄

Nb–Te(1)	2.911(3)	Nb...Fe	2.108(4) ^b
Nb–Te(2)	2.748(2)	Nb–Fe	2.561(3) × 2
Nb–Te(2)	3.109(2)	Nb–Fe	2.798(4) × 2
Nb–Te(3)	2.661(2)	Nb...Fe	3.153(4) ^b
Nb–Te(3)	2.858(2)	Nb–Cu	2.76(1)
Nb–Te(3)	3.033(2)	Nb...Nb	3.046(4) ^b
		Nb–Nb	3.095(4)
		Nb...Nb	3.289(4) ^c
Cu–Te(1)	2.40(1)		
Cu–Te(3)	2.42(1)		
Cu–Te(3)	2.487(8) × 2	Fe–Te(1)	2.540(3) × 2
Cu...Cu	2.62(2) ^a × 2	Fe–Te(2)	2.549(5)
		Fe–Te(3)	2.673(5)
Nb...Nb	0.551(4) ^b		
Fe...Fe	1.110(9) ^b		

^a Distance between two Cu sites, only one of which is occupied.

^b Distance between two sites, only one of which is occupied, due to the positional disorder of the Nb and Fe atoms. ^c The nearest Nb–Nb distance between two adjacent "Nb₄Fe₂Cu₂Te₁₁" building units along the *b*-axis.

would be "Nb₄Fe₂Cu₂Te₁₁", as illustrated in Figure 1a. In this model, the Nb atoms are six-coordinated by Te, forming distorted octahedra with Nb–Te bond distances in the range 2.661(2)–3.109(2) Å (average 2.887 Å). The Fe and Cu atoms are tetrahedrally coordinated, giving the Fe–Te and Cu–Te interatomic distances of 2.540(3)–2.673(3) Å (average 2.576 Å) and 2.40(1)–2.487(8) Å (average 2.45 Å), respectively. The tetrahedral coordination of the Cu suggests a 3d¹⁰ configuration, which is consistent with Cu(I) observed in many of the ternary and quaternary Cu-containing chalcogenides.¹²

The partial occupancy (0.478) of the Nb atom and the extremely short Nb–Nb distance (0.551(4) Å) in the [010] direction suggest that the Nb atoms are positionally disordered over the two general positions 8g about *y* = 0.75. These two positions can never be simultaneously occupied. Similarly, the partial occupancy of the Fe (0.496) site and the very short Fe–Fe distance (1.110(9) Å) in the [100] direction imply that the Fe atoms are also positionally disordered over two 4f sites about *x* = 0.25 and these two positions are never simultaneously occupied. The disordered positions are given in Figure 1a as Nb(1p)/Nb(1q), Nb(1r)/Nb(1s) for the niobium atoms and Fe(1m)/Fe(1n) for the iron atoms. If both Fe and Nb were ordered, their fixed positions would be Fe(1b), Nb(1n), and Nb(1d), as shown in Figure 1b. However, the Fe(1b) atom in the ordered structure (Figure 1b) is unfavorably coordinated by three Te atoms (Te(2d), Te(1d), and Te(1l) (not shown)). This suggests that the positional disorder of the Fe atoms most likely originates from the structural instability of the three-coordinated Fe(1b) atom. The distance between the disordered Fe(1m) (Figure 1a) and the ordered Nb(1n) (Figure 1b), as well as the distance between Fe(1n) and Nb(1d), is only 2.33 Å. This distance is much shorter than the average Nb–Fe bond distance of 2.67 Å (calculated from the

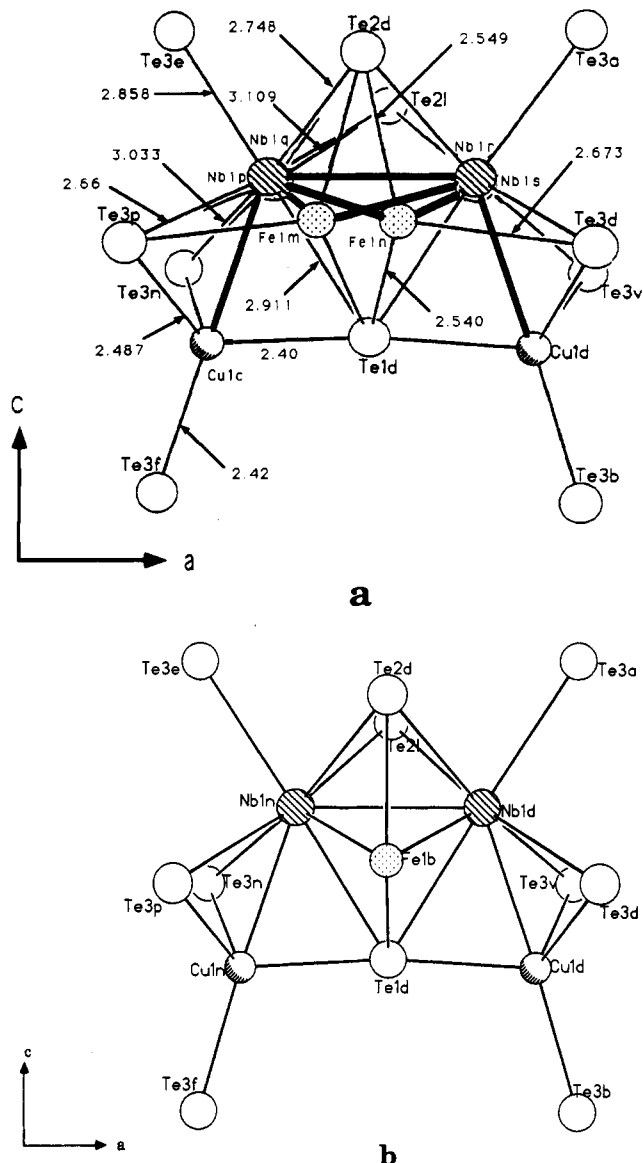


Figure 1. Perspective view of the "Nb₄Fe₂Cu₂Te₁₁" structural building unit of Nb₂FeCu_{0.35}Te₄: (a) The observed structural unit showing the positional disorder of Nb and Fe atoms; all metal–metal bonds are drawn with heavy lines. (b) The ordered, idealized unit. The Nb atoms are represented by the shaded circles, Fe atoms by dotted circles, Cu atoms by partially shaded circles, and Te atoms by open circles. For clarity, the Fe-bonded Te(1) atom in the adjacent unit along [010] is not shown.

Fe–Fe and Nb–Nb metal–metal bond distances),¹³ and the strong electrostatic repulsions lead to the positional disorder of the Nb atoms (as shown in Figure 1a).

As shown in Figure 2, the "Nb₄Fe₂Cu₂Te₁₁" building units are interconnected via the Nb–Te(3) bonds (2.858(2) Å) to form an infinite zigzag chain running along the *a*-axis, which in turn stack on top of each other along the *b*-axis to generate a zigzag sheet that is parallel to the *ab*-plane. The interlayer connections between these zigzag sheets are made through Cu–Te(3) (2.42(1) Å) bonds. The tunnels thus formed are extended along the [010] direction with an approximate dimensions of 3.8 Å (between Te(1) and Te(2), parallel to the *c*-axis) by 6.16 Å (between Te(3) and Te(3), parallel to the *a*-axis).

Most of the known ternary group V transition metal tellurides are layered compounds. Only a few have a three-dimensional network.³⁸ Clearly, the Nb₂FeCu_{0.35}Te₄ structure would be a two-dimensional layered type if the Cu atoms were absent.

(12) See for example: Kanatzidis, M. G.; Park, Y. *J. Am. Chem. Soc.* **1989**, *111*, 3767. Keane, P. M.; Ibers, J. A. *Inorg. Chem.* **1991**, *30*, 3096. Park, Y.; Degroot, D. C.; Schindler, J.; Kannewurf, C. R.; Kanatzidis, M. G. *Angew. Chem., Int. Ed. Engl.* **1991**, *30*, 1325. Keane, P. M.; Ibers, J. A. *J. Solid State Chem.* **1991**, *93*, 291. Park, Y.; Kanatzidis, M. G. *Chem. Mater.* **1991**, *3*, 781. Hirpo, W.; Dhingra, S.; Sutorik, C.; Kanatzidis, M. G. *J. Am. Chem. Soc.* **1993**, *115*, 1597.

(13) Slater, J. C. *Quantum Theory of Molecules and Solids: Symmetry and Energy Bands in Crystals*; Vol. 2, McGraw-Hill Publishers: New York, 1965; p 307.

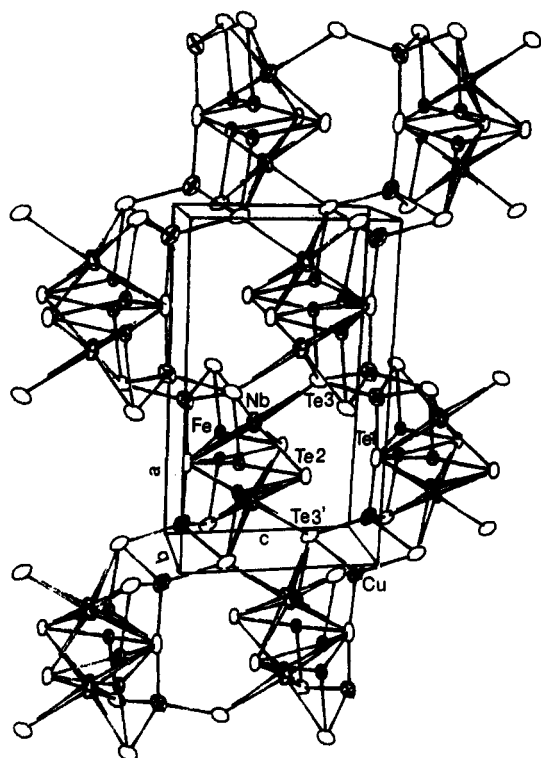


Figure 2. ORTEP drawing (50% thermal ellipsoids) of the $\text{Nb}_2\text{FeCu}_{0.35}\text{Te}_4$ structure, showing the interconnection of the structural building units on the ac -plane. The metal-metal bonds are not shown.

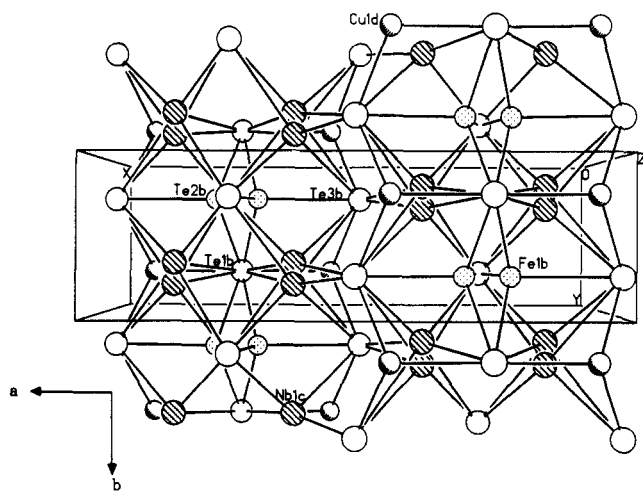


Figure 3. Perspective view of the $\text{Nb}_2\text{FeCu}_{0.35}\text{Te}_4$ structure along the c -axis, illustrating the coordination geometry of the Te atoms. The metal-metal bonds are eliminated for clarity.

However, the Cu sites in this structure are partially occupied, giving an occupancy of 0.174 (i.e. one Cu atom for every six Cu sites). The cause for such a partial occupancy is not yet clear but is unlikely due to structural effects. Whether it is a consequence of electronic effects needs to be explored and might be understood by electronic band calculations.

There are three crystallographically nonequivalent Te atoms in this structure as shown in Figure 3. The Te(1) atom is five-coordinated due to the partial occupancies of Fe (0.496), Nb (0.478), and Cu (0.174). Ideally (i.e., if all metal sites were fully occupied), Te(1) would have made nearest-neighbor contacts to four Fe (2.540(3) Å × 4), four Nb (2.911(3) Å × 4) and two Cu (2.40(1) Å × 2) sites. Similarly, the Te(2) atom is five-coordinated and would make nearest-neighbor contacts to eight disordered Nb (2.748(2) Å × 4 and 3.109(2) Å × 4) and two disordered Fe (2.549(5) Å) sites. The Te(3) atom is analogously five-coordinated with three nearest-neighbor contacts to Cu

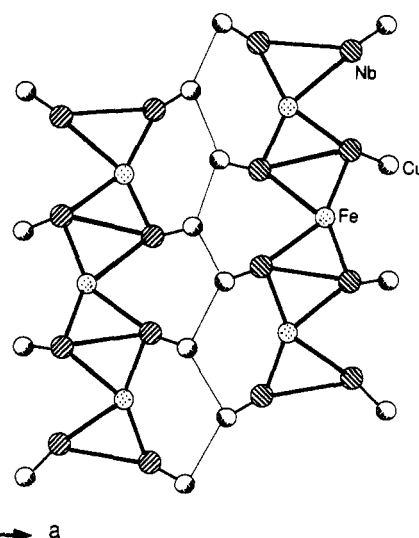
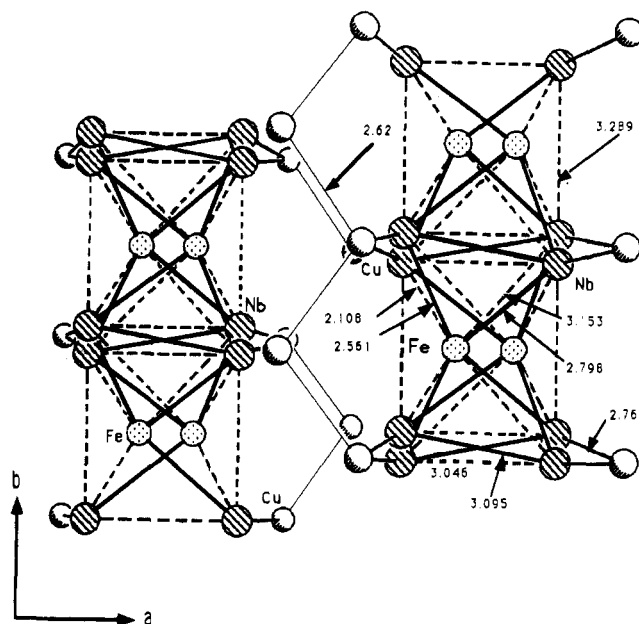


Figure 4. (a) Top: Perspective view of the $\text{Nb}_2\text{FeCu}_{0.35}\text{Te}_4$ structure along the c -axis, showing the extended metal network. The metal-metal bonds are represented by the heavy solid lines, and the nonbonding contacts, by dashed lines. The shortest Cu-Cu contacts are represented by the light solid lines. (b) Bottom: The same view based on a supercell with doubled b axis, which shows the ordered Nb and Fe atoms.

(2.42(1) Å and 2.487(8) Å × 2), one to the disordered Fe (2.673(5) Å) and six to the disordered Nb (2.661(2) Å × 2, 2.858(2) Å × 2, and 3.033(2) Å × 2) sites.

The extended metal networks observed in $\text{Nb}_2\text{FeCu}_{0.35}\text{Te}_4$ are depicted in Figure 4a. All metal-metal contacts are drawn in the figure, including those between disordered positions. The extended metal-metal bonding in $\text{Nb}_2\text{FeCu}_{0.35}\text{Te}_4$ is one-dimensional (along the b -axis) and constrained in the "Nb₄Fe₂Cu₂Te₁₁" building units. The shortest "contact" (2.62(2) Å) between Cu atoms on adjacent units cannot lead to a Cu-Cu bond because of its low occupancy ($\sim 1/6$). If both Nb and Fe atoms were ordered (as illustrated in Figure 1b), the local Fe-to-Nb coordination would have been four-coordinated, as shown in Figure 4b. Upon disorder, each Fe makes contacts to eight disordered Nb positions (2.561(3) Å × 2, 2.798(4) Å × 2, 2.108(4) Å × 2, and 3.153(4) Å × 2). In a similar way, the ordered four-coordinated Nb atom (Figure 4b) becomes disordered to have four contacts to the disordered Fe with the distances listed above, one to Cu (2.76(1) Å) and two to the disordered Nb (3.046 and 3.095 Å) sites. The Cu to Nb distance is 2.76(1) Å.

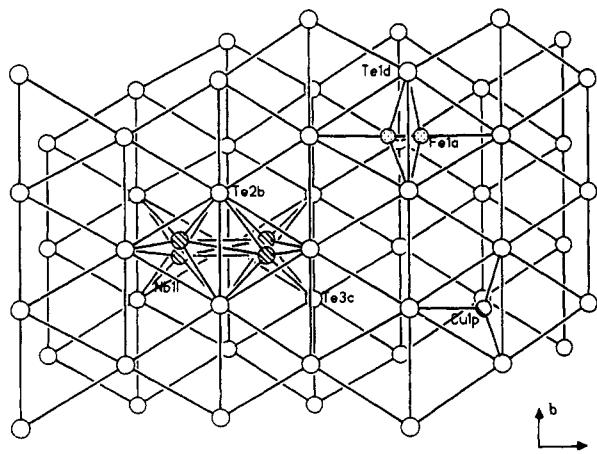


Figure 5. Te sublattice in Nb₂FeCu_{0.35}Te₄ viewed along the *c*-axis showing two single layers of the pucker hexagonal close-packed lattice.

The positional disorder of Nb and Fe and the integral proportion of Nb, Fe, and Te in this formula strongly suggest that Nb and/or Fe might be ordered with a supercell doubling the *b*- and/or *a*-axis. We indeed observed supercell reflections along the *b*-axis (the needle axis) on an oscillation photograph of a crystal with the approximate dimensions of 0.9 × 0.1 × 0.05 mm³ exposed to Cu K α radiation for 12 h. However, the zero- and first-level Weissenberg photographs did not indicate any supercell along the *a*- and *c*-axes.

As in a number of known ternary telluride compounds,^{3f-h} the stacking pattern of the tellurium atoms in Nb₂FeCu_{0.35}Te₄ is highly distorted from the hexagonal close-packed (hcp) lattice observed in NbTe₂.¹⁴ Both A and B layers of the hcp lattice are puckered in such a way that the atoms from the two layers almost line up along the *b*-axis. This is illustrated in Figure 5. The octahedral and tetrahedral interstices defined in the usual sense no longer exist, or they are so distorted that the two become indistinguishable. A structural disorder may therefore be necessary to accommodate the counterions (i.e. Fe, Nb, and Cu), while preserving their preferential coordination (6 and 4 for Nb and Fe, respectively) environment to the Te anions. As indicated in Figures 1a and 5, Fe undergoes such a disorder to ensure its tetrahedral coordination to Te. Consequently, the Nb atom is positionally disordered due to the strong electrostatic repulsion by Fe. It would be interesting to perform an electronic band calculation to study this order-disorder phenomenon.

Magnetic and Electrical Properties. The temperature dependence of the magnetic susceptibility of Nb₂FeCu_{0.35}Te₄ is presented in Figure 6. The susceptibility values were not corrected for the core diamagnetism of the component ions because of their negligible contribution to the total susceptibility of the sample. A well-defined maximum in the susceptibility at 8 K is indicative of the onset of a long-range antiferromagnetic (AF) ordering. The magnetic susceptibility is observed to obey a modified Curie-Weiss relation in the temperature range 20–370 K, according to the equation

$$\chi = \chi_0 + C/(T - \theta)$$

Here χ_0 , C , and θ refer to the temperature-independent contributions (such as Van Vleck, Landau, Larmor, and Pauli magnetisms), Curie constant, and the Curie-Weiss temperature, respectively. A nonlinear least-squares fitting of the observed data to the above equation yielded $\chi_0 = 1.17 \times 10^{-4}$ emu/mol, $C = 0.20$ emu·K/mol, and $\theta = -4.7$ K. A plot of $1/(\chi - \chi_0)$ as a function of temperature is linear in the range 20–370 K (insert of Figure 6) confirming the validity of the above relation.

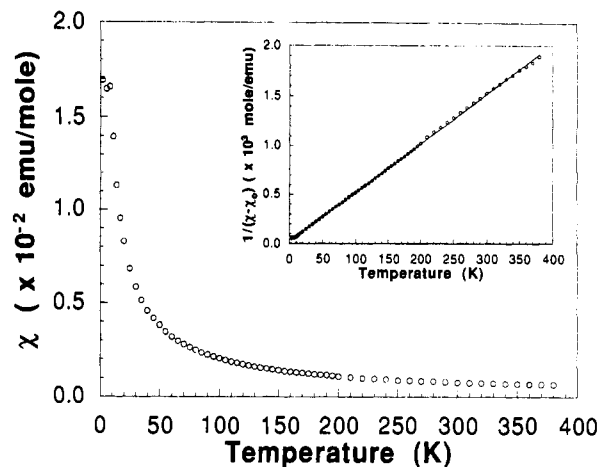


Figure 6. Magnetic susceptibility of Nb₂FeCu_{0.35}Te₄ as a function of temperature. The inset shows the temperature variation of the inverse susceptibility corrected for the χ_0 terms.

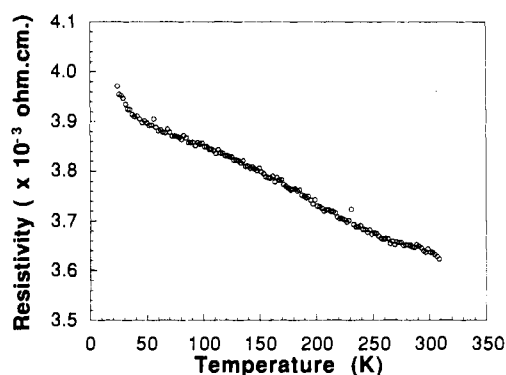


Figure 7. Temperature-dependent electrical resistivity of Nb₂FeCu_{0.35}Te₄.

Assuming spin-only contributions, the effective magnetic moment (μ_{eff}) in this temperature range is 1.26 μ_B , which is considerably smaller than the value of 1.73 μ_B expected for one localized electron. The observed reduced effective magnetic moment is consistent with the expected high covalency of the metal-tellurium bonds.

The electrical resistivity of Nb₂FeCu_{0.35}Te₄ as a function of temperature is shown in Figure 7. The room-temperature resistivity ($\rho_{300\text{K}}$) of the sample $3.6(2) \times 10^{-3}$ $\Omega\cdot\text{cm}$ increases very slightly as the temperature is lowered to 20 K ($\rho_{20\text{K}} = 3.9(2) \times 10^{-3}$ $\Omega\cdot\text{cm}$). The low resistivity and the small change of ρ with temperature is consistent with the behavior of a degenerate semiconductor (or a poor metal). The observed semiconducting property can be attributed to the following: (a) the positional disorder and low occupancies of the transition metal ions in the structure, which would reduce the effective long-range overlap of the orbitals necessary for metallic conduction, and (b) strong coupling of the magnetic and conduction electrons as has been proposed for the corresponding ternary composition NbFeTe₂.^{3f}

Conclusion

Nb₂FeCu_{0.35}Te₄, the first solid-state quaternary niobium telluride, has been synthesized via vapor transport reactions. The crystal structure has been determined by single-crystal X-ray diffraction methods. The compound represents a novel 3D structure type with interesting structural features and one-dimensional extended metal-metal bonds. In general, the structure of Nb₂FeCu_{0.35}Te₄ can be best described as composed of layers with two pucker hexagonal Te sheets enclosing octahedrally coordinated Nb. The Nb atoms are arranged in

such a way that they occupy face-sharing pairs of octahedra (Figure 5), each pair sharing edges with adjacent octahedra pairs. These layers are decorated with Fe atoms occupying one quarter of the tetrahedral sites on the surface of the layer. The layers stack along the *c*-axis, linked by a small number of Cu atoms (one for every three formula units). The low effective magnetic moment ($\mu_{\text{eff}} = 1.26 \mu_{\text{B}}$) observed for $\text{Nb}_2\text{FeCu}_{0.35}\text{Te}_4$ is attributed to the high covalency of the metal–tellurium bonds. The degenerate semiconducting behavior seen in the temperature-dependent resistivity of $\text{Nb}_2\text{FeCu}_{0.35}\text{Te}_4$ is most likely due to the disorder and the low occupancies of the transition metal ions. The positional disorder of Nb and Fe atoms, the one-dimensional extended metal–metal network, and the open channels along the

b-axis observed in this unusual structure are quite interesting and deserve further investigations.

Acknowledgment. We thank Reviewer II of our paper; his insightful comments helped improve this manuscript immensely. The work of J.L., F.M., and M.J.D. was supported by the Schering-Plough Award and the Bristol-Myers Squibb Co. Award of the Research Corp. and by the Petroleum Research Fund. The work of S.C.C., K.V.R., and M.G. was supported by the National Science Foundation Solid State Chemistry Grant DMF-90-19301.

Supplementary Material Available: Tables of crystallographic details (Table S1), anisotropic thermal parameters (Table S2), and complete interatomic distances (Table S3) and angles (Table S4) (9 pages). Ordering information is given on any current masthead page.